A new method of designing complementary filters for sensor fusion using $\mathcal{H}_\infty$ synthesis

Thomas Dehaeze[a,b,*], Mohit Verma[c,d], Christophe Collette[b,d]

[a] *European Synchrotron Radiation Facility, Grenoble, France*
[b] *University of Liège, Department of Aerospace and Mechanical Engineering, 4000 Liège, Belgium.*
[c] *CSIR — Structural Engineering Research Centre, Taramani, Chennai — 600113, India.*
[d] *Université Libre de Bruxelles, Precision Mechatronics Laboratory, BEAMS Department, 1050 Brussels, Belgium.*

Abstract

Sensor have limited bandwidth and are accurate only in a certain frequency band. In many applications, the signals of different sensor are fused together in order to either enhance the stability or improve the operational bandwidth of the system. The sensor signals can be fused using complementary filters. The tuning of complementary filters is a complex task and is the subject of this paper. The filters needs to meet design specifications while satisfying the complementary property. This paper presents a framework to shape the norm of complementary filters using the $\mathcal{H}_\infty$ norm minimization. The design specifications are imposed as constraints in the optimization problem by appropriate selection of weighting functions. The proposed method is quite general and easily extendable to cases where more than two sensors are fused. Finally, the proposed method is applied to the design of complementary filter design for active vibration isolation of the Laser Interferometer Gravitation-wave Observatory (LIGO).

Keywords: Sensor fusion, Optimal filters, $\mathcal{H}_\infty$ synthesis, Vibration isolation, Precision

1. Introduction

- [1] roots of sensor fusion
- Increase the bandwidth: [2]
- Increased robustness: [3]
- Decrease the noise:
- UAV: [4], [5]
- Gravitational wave observer: [6, 7]
- [8] alternate form of complementary filters => Kalman filtering
- [9] Compare Kalman Filtering with sensor fusion using complementary filters
- [10] advantage of complementary filters over Kalman filtering
- [4] use LMI to generate complementary filters
- [11] use H-Infinity to optimize complementary filters (flatten the super sensor noise spectral density)
- [5] design of complementary filters with classical control theory
- [6, 7]: FIR + convex optimization
- 3 complementary filters: [12]
- Analytical methods:

*Corresponding author. Email Address: dehaeze.thomas@gmail.com

- first order: [13]
- second order: [14], [15], [5]
- higher order: [16], [2], [3], [17]

- Analog complementary filters: [18], [19]
- Robustness problems: [2] change of phase near the merging frequency
- Trial and error
- Although many design methods of complementary filters have been proposed in the literature, no simple method that allows to shape the norm of the complementary filters is available.

2. Complementary Filters Requirements

2.1. Sensor Fusion Architecture

Let's consider two sensors measuring the same physical quantity x with dynamics $G_1(s)$ and $G_2(s)$, and with uncorrelated noise characteristics n_1 and n_2.

The signals from both sensors are fed into two complementary filters $H_1(s)$ and $H_2(s)$ and then combined to yield an estimate $\hat{x}$ of x as shown in Fig. 1.

$$\hat{x} = (G_1 H_1 + G_2 H_2)\, x + H_1 n_1 + H_2 n_2 \tag{1}$$

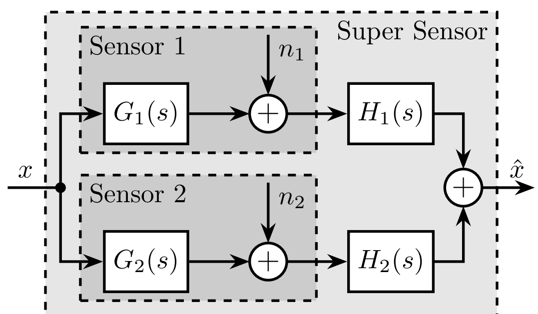

Figure 1: Sensor fusion architecture

The complementary property of $H_1(s)$ and $H_2(s)$ implies that their transfer function sum is equal to one at all frequencies (2).

$$H_1(s) + H_2(s) = 1 \tag{2}$$

2.2. Noise Sensor Filtering

Let's first consider sensors with perfect dynamics

$$G_1(s) = G_2(s) = 1 \tag{3}$$

The estimate $\hat{x}$ is then described by

$$\hat{x} = x + H_1 n_1 + H_2 n_2 \tag{4}$$

From (4), the complementary filters $H_1(s)$ and $H_2(s)$ are shown to only operate on the sensor's noise. Thus, this sensor fusion architecture permits to filter the noise of both sensors without introducing any distortion in the physical quantity to be measured.

Let's define the estimation error δx by (5).

$$\delta x \triangleq \hat{x} - x = H_1 n_1 + H_2 n_2 \tag{5}$$

As shown in (6), the Power Spectral Density (PSD) of the estimation error $\Phi_{\delta x}$ depends both on the norm of the two complementary filters and on the PSD of the noise sources Φ_{n_1} and Φ_{n_2}.

$$\Phi_{\delta x} = \left|H_1\right|^2 \Phi_{n_1} + \left|H_2\right|^2 \Phi_{n_2} \tag{6}$$

Usually, the two sensors have high noise levels over distinct frequency regions. In order to lower the noise of the super sensor, the value of the norm $|H_1|$ has to be lowered when Φ_{n_1} is larger than Φ_{n_2} and that of $|H_2|$ lowered when Φ_{n_2} is larger than Φ_{n_1}.

2.3. Robustness of the Fusion

In practical systems the sensor dynamics is not perfect and (3) is not verified. In such case, one can use an inversion filter $\hat{G}_i^{-1}(s)$ to normalize the sensor dynamics, where $\hat{G}_i(s)$ is an estimate of the sensor dynamics $G_i(s)$. However, as there is always some level of uncertainty on the dynamics, it cannot be perfectly inverted and $\hat{G}_i^{-1}(s)G_i(s) \neq 1$.

Let's represent the resulting dynamic uncertainty of the inverted sensors by an input multiplicative uncertainty as shown in Fig. 2 where Δ_i is any stable transfer function satisfying $|\Delta_i(j\omega)| \leq 1,\ \forall\omega$, and $|w_i(s)|$ is a weight representing the magnitude of the uncertainty.

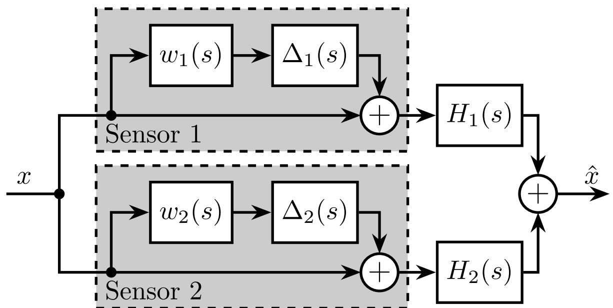

Figure 2: Sensor fusion architecture with sensor dynamics uncertainty

The super sensor dynamics (7) is no longer equal to 1 and now depends on the sensor dynamics uncertainty weights $w_i(s)$ as well as on the complementary filters $H_i(s)$.

$$\frac{\hat{x}}{x} = 1 + w_1(s)H_1(s)\Delta_1(s) + w_2(s)H_2(s)\Delta_2(s) \tag{7}$$

The uncertainty region of the super sensor can be represented in the complex plane by a circle centered on 1 with a radius equal to $|w_1(j\omega)H_1(j\omega)| + |w_2(j\omega)H_2(j\omega)|$ as shown in Fig. 3.

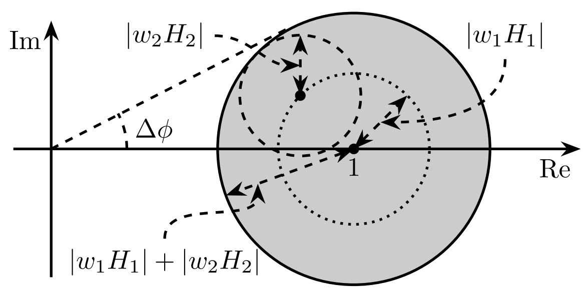

Figure 3: Uncertainty region of the super sensor dynamics in the complex plane (solid circle). The contribution of both sensors 1 and 2 to the uncertainty are represented respectively by a dotted and a dashed circle

The maximum phase added $\Delta\phi(\omega)$ by the super sensor dynamics at frequency ω is then

$$\Delta\phi(\omega) = \arcsin\big(|w_1(j\omega)H_1(j\omega)| + |w_2(j\omega)H_2(j\omega)|\big) \tag{8}$$

As it is generally desired to limit the maximum phase added by the super sensor, $H_1(s)$ and $H_2(s)$ should be designed such that (9) is satisfied.

$$\max_\omega \big(\, |w_1H_1| + |w_2H_2| \,\big) < \sin\left(\Delta\phi_{\max}\right) \tag{9}$$

where $\Delta\phi_{\max}$ is the maximum allowed added phase.

Thus the norm of the complementary filter $|H_i|$ should be made small at frequencies where $|w_i|$ is large.

3. Complementary Filters Shaping using $\mathcal{H}_\infty$ Synthesis

As shown in Sec. 2, the performance and robustness of the sensor fusion architecture depends on the complementary filters norms. Therefore, the development of a synthesis method of complementary filters that allows the shaping of their norm is necessary.

3.1. *Shaping of Complementary Filters using $\mathcal{H}_\infty$ synthesis*

The synthesis objective is to shape the norm of two filters $H_1(s)$ and $H_2(s)$ while ensuring their complementary property (2). This is equivalent as to finding stable transfer functions $H_1(s)$ and $H_2(s)$ such that conditions (10) are satisfied.

$$H_1(s) + H_2(s) = 1 \tag{10a}$$

$$|H_1(j\omega)| \le \frac{1}{|W_1(j\omega)|} \quad \forall\omega \tag{10b}$$

$$|H_2(j\omega)| \le \frac{1}{|W_2(j\omega)|} \quad \forall\omega \tag{10c}$$

where $W_1(s)$ and $W_2(s)$ are two weighting transfer functions that are chosen to shape the norms of the corresponding filters.

In order to express this optimization problem as a standard $\mathcal{H}_\infty$ problem, the architecture shown in Fig. 4 is used where the generalized plant P is described by (11).

$$\begin{bmatrix} z_1 \\ z_2 \\ v \end{bmatrix} = P(s) \begin{bmatrix} w \\ u \end{bmatrix}; \quad P(s) = \begin{bmatrix} W_1(s) & -W_1(s) \\ 0 & W_2(s) \\ 1 & 0 \end{bmatrix} \tag{11}$$

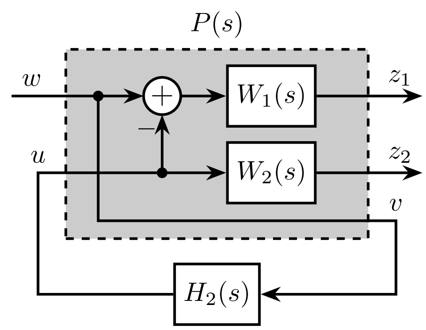

Figure 4: Architecture used for $\mathcal{H}_\infty$ synthesis of complementary filters

The $\mathcal{H}_\infty$ filter design problem is then to find a stable filter $H_2(s)$ which based on v, generates a signal u such that the $\mathcal{H}_\infty$ norm from w to $[z_1,\ z_2]$ is less than one (12).

$$\left\| \begin{matrix} [1 - H_2(s)]\, W_1(s) \\ H_2(s) W_2(s) \end{matrix} \right\|_\infty \le 1 \tag{12}$$

This is equivalent to having (13) by defining $H_1(s)$ as the complementary filter of $H_2(s)$ (14).

$$\left\| \begin{matrix} H_1(s) W_1(s) \\ H_2(s) W_2(s) \end{matrix} \right\|_\infty \le 1 \tag{13}$$

$$H_1(s) \triangleq 1 - H_2(s) \tag{14}$$

The complementary condition (10a) is ensured by (14). The conditions (10b) and (10c) on the filters shapes are satisfied by (13). Therefore, all the conditions (10) are satisfied using this synthesis method based on $\mathcal{H}_\infty$ synthesis, and thus it permits to shape complementary filters as desired.

3.2. *Weighting Functions Design*

The proper design of the weighting functions is of primary importance for the success of the presented complementary filters $\mathcal{H}_\infty$ synthesis.

First, only proper, stable and minimum phase transfer functions should be used. Second, the order of the weights should stay reasonably small in order to reduce the computational costs associated with the solving of the optimization problem and for the physical implementation of the filters (the order of the synthesized filters being equal to the sum of the weighting functions order). Third, one should not forget the fundamental limitations imposed by the complementary property (2). This implies for instance that $|H_1(j\omega)|$ and $|H_2(j\omega)|$ cannot be made small at the same time.

When designing complementary filters, it is usually desired to specify the slope of the filter, its crossover frequency and its gain at low and high frequency. To help with the design of the weighting functions such that the above specification can be easily expressed, the following formula is proposed.

$$W(s) = \left(\frac{\frac{1}{\omega_0} \sqrt{\frac{1-\left(\frac{G_0}{G_c}\right)^{\frac{2}{n}}}{1-\left(\frac{G_c}{G_\infty}\right)^{\frac{2}{n}}}} s + \left(\frac{G_0}{G_c}\right)^{\frac{1}{n}}}{\left(\frac{1}{G_\infty}\right)^{\frac{1}{n}} \frac{1}{\omega_0} \sqrt{\frac{1-\left(\frac{G_0}{G_c}\right)^{\frac{2}{n}}}{1-\left(\frac{G_c}{G_\infty}\right)^{\frac{2}{n}}}} s + \left(\frac{1}{G_c}\right)^{\frac{1}{n}}} \right)^n \tag{15}$$

The parameters permit to specify:

- the low frequency gain: $G_0 = lim_{\omega \to 0} |W(j\omega)|$
- the high frequency gain: $G_\infty = lim_{\omega \to \infty} |W(j\omega)|$
- the absolute gain at ω_0: $G_c = |W(j\omega_0)|$
- the absolute slope between high and low frequency: n

The parameters G_0, G_c and G_∞ should either satisfy condition (16a) or (16b).

$$G_0 < 1 < G_\infty \text{ and } G_0 < G_c < G_\infty \tag{16a}$$
$$G_\infty < 1 < G_0 \text{ and } G_\infty < G_c < G_0 \tag{16b}$$

The general shape of a weighting function generated using (15) is shown in Fig. 5.

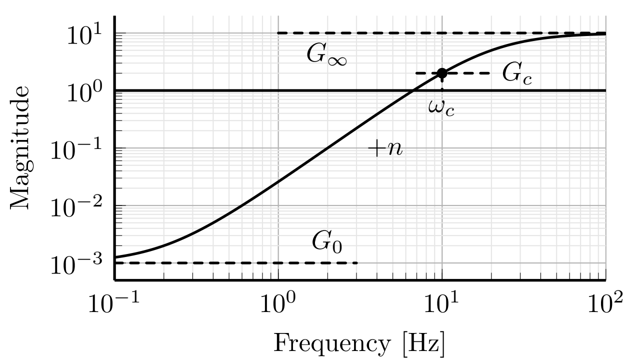

Figure 5: Magnitude of a weighting function generated using the proposed formula (15), $G_0 = 1e^{-3}$, $G_\infty = 10$, $\omega_c = 10\,\text{Hz}$, $G_c = 2$, $n = 3$

3.3. *Validation of the proposed synthesis method*

Let's validate the proposed design method of complementary filters with a simple example where two complementary filters $H_1(s)$ and $H_2(s)$ have to be designed such that:

- the merging frequency is around 10 Hz
- the slope of $|H_1(j\omega)|$ is -2 above 10 Hz
- the slope of $|H_2(j\omega)|$ is $+3$ below 10 Hz
- the gain of both filters is equal to 10^{-3} away from the merging frequency

The weighting functions $W_1(s)$ and $W_2(s)$ are designed using (15). The parameters used are summarized in table 1 and the magnitude of the weighting functions is shown in Fig. 6.

Table 1: Parameters used for $W_1(s)$ and $W_2(s)$

Parameter	$W_1(s)$	$W_2(s)$
G_0	0.1	1000
G_∞	1000	0.1
ω_c [Hz]	11	10
G_c	0.5	0.5
n	2	3

The bode plots of the obtained complementary filters are shown in Fig. 6 and their transfer functions in the Laplace domain are given below.

$$H_1(s) = \frac{10^{-8}(s + 6.6e^9)(s + 3450)^2(s^2 + 49s + 895)}{(s + 6.6e^4)(s^2 + 106s + 3e^3)(s^2 + 72s + 3580)}$$
$$H_2(s) = \frac{(s + 6.6e^4)(s + 160)(s + 4)^3}{(s + 6.6e^4)(s^2 + 106s + 3e^3)(s^2 + 72s + 3580)}$$

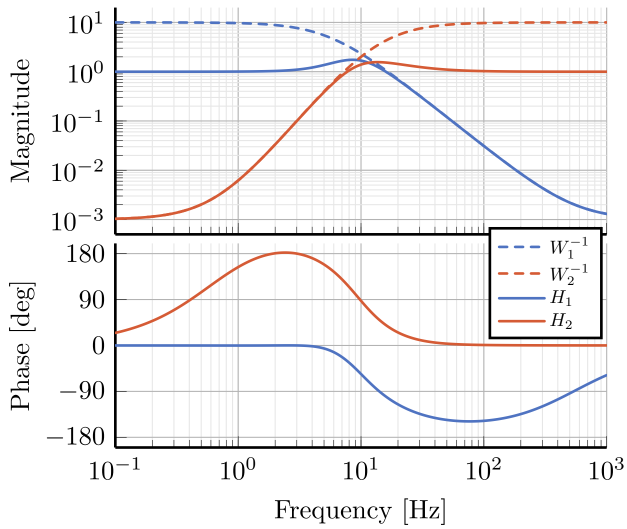

Figure 6: Frequency response of the weighting functions and complementary filters obtained using $\mathcal{H}_\infty$ synthesis

3.4. Synthesis of Three Complementary Filters

Some applications may require to merge more than two sensors. In such a case, it is necessary to design as many complementary filters as the number of sensors used. The synthesis problem is then to compute n stable transfer functions $H_i(s)$ such that (17) is satisfied.

$$\sum_{i=0}^{n} H_i(s) = 1 \tag{17a}$$

$$|H_i(j\omega)| < \frac{1}{|W_i(j\omega)|}, \quad \forall \omega, \ i = 1 \dots n \tag{17b}$$

The synthesis method is generalized here for the synthesis of three complementary filters using the architecture shown in Fig. 7.

The $\mathcal{H}_\infty$ synthesis objective applied on $P(s)$ is to design two stable filters $H_2(s)$ and $H_3(s)$ such that the $\mathcal{H}_\infty$ norm of the transfer function from w to $[z_1, \ z_2, \ z_3]$ is less than one (18).

$$\left\| \begin{matrix} [1 - H_2(s) - H_3(s)]\, W_1(s) \\ H_2(s) W_2(s) \\ H_3(s) W_3(s) \end{matrix} \right\|_\infty \leq 1 \tag{18}$$

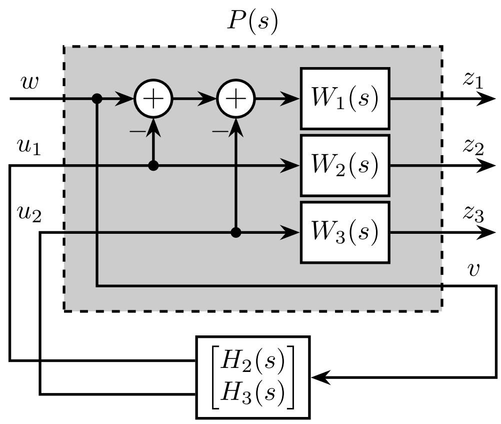

Figure 7: Architecture for $\mathcal{H}_\infty$ synthesis of three complementary filters

By choosing $H_1(s) \triangleq 1 - H_2(s) - H_3(s)$, the proposed $\mathcal{H}_\infty$ synthesis solves the design problem (17).

An example is given to validate the method where three sensors are used in different frequency bands (up to 1 Hz, from 1 to 10 Hz and above 10 Hz respectively). Three weighting functions are designed using (15) and shown by dashed curves in Fig. 8. The bode plots of the obtained complementary filters are shown in Fig. 8.

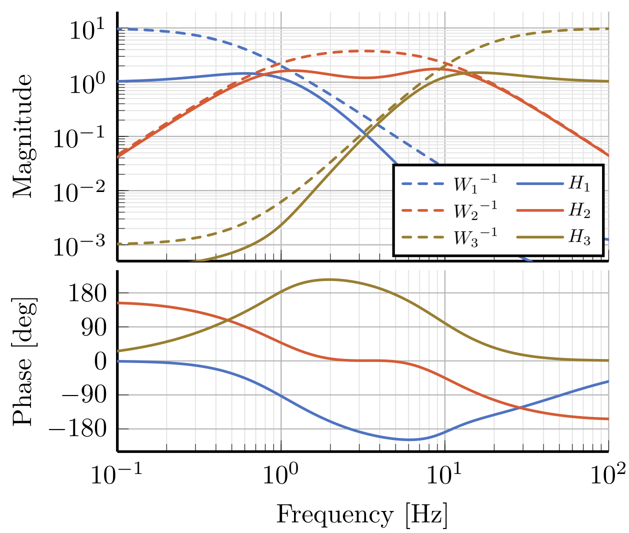

Figure 8: Frequency response of the weighting functions and three complementary filters obtained using $\mathcal{H}_\infty$ synthesis

4. Application: Design of Complementary Filters used in the Active Vibration Isolation System at the LIGO

Several complementary filters are used in the active isolation system at the LIGO [6, 7]. The requirements on those filters are very tight and thus their design is complex. The approach used in [6] for their design is to write the synthesis of complementary FIR filters as a convex optimization problem. The obtained FIR filters are compliant with the requirements. However they are of very high order so their implementation is quite complex.

The effectiveness of the proposed method is demonstrated by designing complementary filters with the same requirements as the one described in [6].

4.1. Complementary Filters Specifications

The specifications for one pair of complementary filters used at the LIGO are summarized below (for further details, refer to [7]) and shown in Fig. 9:

- From 0 to 0.008 Hz, the magnitude of the filter's transfer function should be less or equal to 8×10^{-4}

- Between 0.008 Hz to 0.04 Hz, the filter should attenuate the input signal proportional to frequency cubed
- Between 0.04 Hz to 0.1 Hz, the magnitude of the transfer function should be less than 3
- Above 0.1 Hz, the magnitude of the complementary filter should be less than 0.045

4.2. Weighting Functions Design

The weighting functions should be designed such that their inverse magnitude is as close as possible to the specifications in order to not over-constrain the synthesis problem. However, the order of each weight should stay reasonably small in order to reduce the computational costs of the optimization problem as well as for the physical implementation of the filters.

A Type I Chebyshev filter of order 20 is used as the weighting transfer function $w_L(s)$ corresponding to the low pass filter. For the one corresponding to the high pass filter $w_H(s)$, a 7^{th} order transfer function is designed. The magnitudes of the weighting functions are shown in Fig. 9.

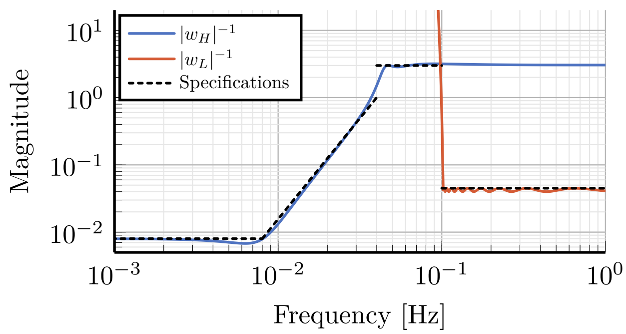

Figure 9: Specifications and weighting functions magnitudes

4.3. $\mathcal{H}_\infty$ Synthesis

$\mathcal{H}_\infty$ synthesis is performed using the architecture shown in Fig. 11. The complementary filters obtained are of order 27. In Fig. 10, their bode plot is compared with the FIR filters of order 512 obtained in [6]. They are found to be very close to each other and this shows the effectiveness of the proposed synthesis method.

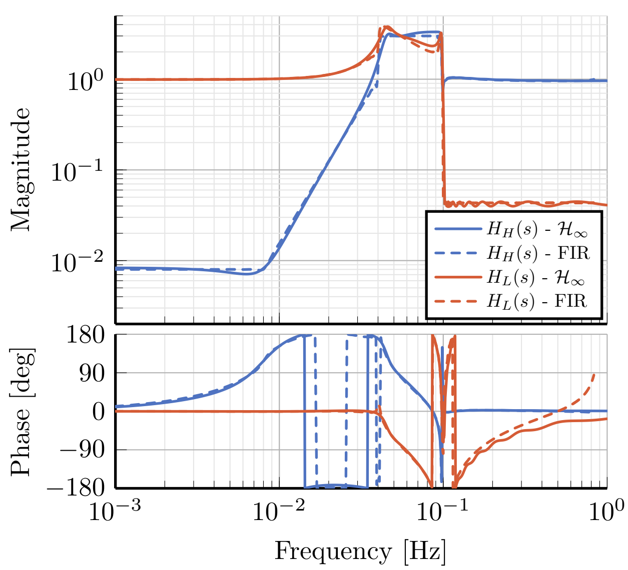

Figure 10: Comparison of the FIR filters (solid) designed in [6] with the filters obtained with $\mathcal{H}_\infty$ synthesis (dashed)

5. Conclusion

This paper has shown how complementary filters can be used to combine multiple sensors in order to obtain a super sensor. Typical specification on the super sensor noise and on the robustness of the sensor fusion has been shown to be linked to the norm of the complementary filters. Therefore, a synthesis method that permits the shaping of the complementary filters norms has been proposed and has been successfully applied for the design of complex filters. Future work will aim at further developing this synthesis method for the robust and optimal synthesis of complementary filters used in sensor fusion.

Acknowledgment

This research benefited from a FRIA grant from the French Community of Belgium.

References

[1] J. Bendat, Optimum filters for independent measurements of two related perturbed messages, IRE Transactions on Circuit Theory (1957). doi:10.1109/tct.1957.1086345.
URL https://doi.org/10.1109/tct.1957.1086345

[2] M. Zimmermann, W. Sulzer, High bandwidth orientation measurement and control based on complementary filtering, Robot Control 1991 (1992) 525–530doi:10.1016/B978-0-08-041276-4.50093-5.
URL https://doi.org/10.1016/B978-0-08-041276-4.50093-5

[3] C. Collette, F. Matichard, Sensor fusion methods for high performance active vibration isolation systems, Journal of Sound and Vibration 342 (2015) 1–21. doi:10.1016/j.jsv.2015.01.006.
URL https://doi.org/10.1016/j.jsv.2015.01.006

[4] A. Pascoal, I. Kaminer, P. Oliveira, Navigation system design using time-varying complementary filters, in: Guidance, Navigation, and Control Conference and Exhibit, 1999. doi:10.1109/7.892661.
URL https://doi.org/10.1109/7.892661

[5] A. Jensen, C. Coopmans, Y. Chen, Basics and guidelines of complementary filters for small uas navigation, in: 2013 International Conference on Unmanned Aircraft Systems (ICUAS), 2013. doi:10.1109/ICUAS.2013.6564726.
URL https://doi.org/10.1109/ICUAS.2013.6564726

[6] W. Hua, Low frequency vibration isolation and alignment system for advanced ligo, Ph.D. thesis, stanford university (2005). doi:10.1117/12.552518.
URL https://doi.org/10.1117/12.552518

[7] W. Hua, B. Debra, T. Hardham, T. Lantz, A. Giaime, Polyphase fir complementary filters for control systems, in: Proceedings of ASPE Spring Topical Meeting on Control of Precision Systems, 2004, pp. 109–114.

[8] R. G. Brown, Integrated navigation systems and kalman filtering: a perspective, Navigation 19 (4) (1972) 355–362. doi:10.1002/j.2161-4296.1972.tb01706.x.
URL https://doi.org/10.1002/j.2161-4296.1972.tb01706.x

[9] W. T. Higgins, A comparison of complementary and kalman filtering, IEEE Transactions on Aerospace and Electronic Systems (3) (1975) 321–325. doi:10.

[10] P. Y. C. H. Robert Grover Brown, Introduction to Random Signals and Applied Kalman Filtering with Matlab Exercises, 4th Edition, Wiley, 2012.

[11] A. Plummer, Optimal complementary filters and their application in motion measurement, Proceedings of the Institution of Mechanical Engineers, Part I: Journal of Systems and Control Engineering 220 (6) (2006) 489–507. doi:10.1243/09596518JSCE229.
URL https://doi.org/10.1243/09596518JSCE229

[12] J. A. O. A. S. d. R. L. P. Becker, Thiago; Fabro, Complementary filter design with three frequency bands: Robot attitude estimation, in: International Conference on Autonomous Robot Systems and Competitions, 2015. doi:10.1109/ICARSC.2015.34.
URL https://doi.org/10.1109/ICARSC.2015.34

[13] P. Corke, An inertial and visual sensing system for a small autonomous helicopter, Journal of Robotic Systems 21 (2) (2004) 43–51. doi:10.1002/rob.10127.
URL https://doi.org/10.1002/rob.10127

[14] A.-J. Baerveldt, R. Klang, A low-cost and low-weight attitude estimation system for an autonomous helicopter, in: Proceedings of IEEE International Conference on Intelligent Engineering Systems, 1997, p. nil. doi:10.1109/ines.1997.632450.
URL https://doi.org/10.1109/ines.1997.632450

[15] D. Stoten, Fusion of kinetic data using composite filters, Proceedings of the Institution of Mechanical Engineers, Part I: Journal of Systems and Control Engineering 215 (5) (2001) 483–497. doi:10.

[16] F. Shaw, K. Srinivasan, Bandwidth enhancement of position measurements using measured acceleration, Mechanical Systems and Signal Processing 4 (1) (1990) 23–38. doi:10.1016/0888-3270(90)90038-M.
URL https://doi.org/10.1016/0888-3270(90)90038-M

[17] F. Matichard, B. Lantz, R. Mittleman, K. Mason, J. Kissel, et al., Seismic isolation of advanced ligo: Review of strategy, instrumentation and performance, Classical and Quantum Gravity 32 (18) (2015) 185003. doi:10.1088/0264-9381/32/18/185003.
URL https://doi.org/10.1088/0264-9381/32/18/185003

[18] Y. K. Yong, A. J. Fleming, High-speed vertical positioning stage with integrated dual-sensor arrangement, Sensors and Actuators A: Physical 248 (2016) 184 – 192. doi:10.1016/j.sna.2016.06.042.
URL https://doi.org/10.1016/j.sna.2016.06.042

[19] S. I. Moore, A. J. Fleming, Y. K. Yong, Capacitive instrumentation and sensor fusion for high-bandwidth nanopositioning, IEEE Sensors Letters 3 (8) (2019) 1–3. doi:10.1109/lsens.2019.2933065.
URL https://doi.org/10.1109/lsens.2019.2933065